HARQ Throughput Performance of Multicode DS-CDMA with MMSE Turbo Equalization

Kazuaki TAKEDA[+] and Fumiyuki ADACHI[++]
Dept. of Electrical and Communication Engineering, Graduate School of Engineering, Tohoku University
6-6-05 Aza-Aoba, Aramaki, Aoba-ku, Sendai, 980-8579 Japan
E-mail: [+]takeda@mobile.ecei.tohoku.ac.jp, [++]adachi@ecei.tohoku.ac.jp

***Abstract*—Hybrid automatic repeat request (HARQ) is an indispensable technique for packet access. This is employed in high speed downlink packet access (HSDPA) using the orthogonal multicode direct sequence code division multiple access (DS-CDMA). As the data rate increases, the frequency-selectivity of the channel becomes severer and some equalization technique other than rake combining is necessary. The use of MMSE frequency-domain equalization (MMSE-FDE) can significantly improve the throughput performance. However, the residual inter-chip-inference (ICI) after MMSE-FDE produces the orthogonality distortion among the spreading codes and the throughput performance is far from the theoretical lower bound. In this paper, we study an MMSE turbo equalization for HARQ using multicode DS-CDMA. It is shown by computer simulation that MMSE turbo equalization can significantly improve the throughput performance. An E_s/N_0 reduction of as much as 2.5~3 dB from the no turbo equalization case is obtained for a throughput range of 2~2.5 bit/s/Hz.**

Keywords-component; DS-CDMA; Frequency-domain equalization; MMSE turbo equalization

I. Introduction

With the growing market of mobile wireless communications, high speed and high quality data transmissions are demanded. The high speed packet access will dominate in the next generation IP-based wireless communication systems. Hybrid automatic repeat request (HARQ) is an indispensable technique [1] and is used for high speed downlink packet access (HSDPA) [2]. HSDPA is based on the orthogonal multicode direct sequence code division multiplex access (DS-CDMA). Since the wireless channel is frequency-selective [3], some equalization technique is necessary. For the data transmissions of around a few Mbps, rake combining is used to combat with the frequency-selective fading channel [4]-[5]. However, since much higher speed packet data services of around hundreds of Mbps are demanded in the next generation wireless communication systems, the frequency-selectivity of the channel becomes much severer, and hence the throughput performance with rake combining significantly degrades due to a strong inter-path interference (IPI).

Recently, it has been shown [1], [6]-[9] that FDE based on the minimum mean square error (MMSE) criterion can improve the bit error rate (BER)/throughput performance for the multicode DS-CDMA. However, the presence of a residual inter-chip interference (ICI) after FDE distorts the orthogonality among the spreading codes and the throughput performance is far from the theoretical upper bound. Recently, the turbo equalization technique has been drawing attention since it can suppress the interference while achieving high coding gain by iteratively performing channel equalization and channel decoding [10]-[12]. In this paper, we study an MMSE turbo equalization for HARQ using multicode DS-CDMA and evaluate its throughput performance by computer simulation. We consider type I HARQ, where the same packet is re-transmitted for packet combining.

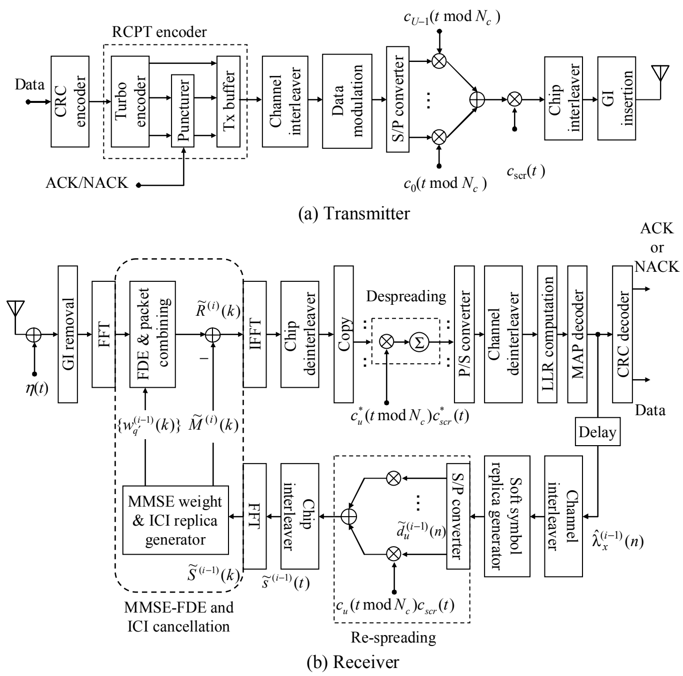

Figure 1. Transmission system model.

II. MMSE Turbo Equalization

The transmission system model for HARQ using multicode DS-CDMA with turbo equalization is illustrated in Fig.1. In MMSE turbo equalization, a series of MMSE-FDE, ICI cancellation and maximum *a posteriori* (MAP) decoding is repeated to sufficiently suppress the residual ICI after FDE and to obtain the higher coding gain. Below, the *i*th iteration is described. Throughout this paper, chip-spaced time representation of the signals is used (the chip duration is denoted by T_c).

A. MMSE-FDE and Packet Combining

We assume that the same packet has been transmitted q times (i.e., the number of retransmissions is q). The received N_c-chip block { $r^{(q)}(t)$; t=0~N_c–1} for the qth packet retransmission is transformed by N_c-point FFT into the frequency-domain signal { $R^{(q)}(k)$; k=0~N_c–1}. $R^{(q)}(k)$ is written as [8]

$$R^{(q)}(k)=\sum_{t=0}^{N_c-1} r^{(q)}(t)\exp\left(-j2\pi k\frac{t}{N_c}\right). \quad (1)$$

Using the past received packets, joint MMSE-FDE and packet combining is carried out as follows:

$$\begin{aligned}\hat{R}^{(i)}(k)&=\sum_{q'=1}^{q} w_{q'}^{(i)}(k)R^{(q')}(k)\\&=S(k)\hat{H}^{(i)}(k)+\hat{\Pi}^{(i)}(k)\end{aligned} \quad (2)$$

with

$$\hat{H}^{(i)}(k)=\sum_{q'=1}^{q} w_{q'}^{(i)}(k)H^{(q')}(k), \quad (3)$$

where $w_{q'}^{(i)}(k)$, $q'=1,2,...,q$, is the equalization weight and will be derived in Sect. III. $H^{(q)}(k)$ is the channel gain for the kth frequency [8] and $\hat{H}^{(i)}(k)$ and $\hat{\Pi}^{(i)}(k)$ are respectively the equivalent channel gain and the noise component. $S(k)$ is the kth frequency component of the transmitted chip sequence {$s(t)$; t=0~N_c–1} and is given by

$$S(k)=\sum_{t=0}^{N_c-1} s(t)\exp\left(-j2\pi k\frac{t}{N_c}\right) \quad (4)$$

with

$$s(t)=\left[\sum_{u=0}^{U-1} d_u\left(\lfloor t/SF\rfloor\right)c_u(t \bmod SF)\right]c_{scr}(t), \quad (5)$$

where U is the code-multiplexing order and { $d_u(m)$; m=0~N_c/SF–1}, u=0~U–1, is the transmitted data symbol sequence for the uth code channel. $c_u(t)$ is an orthogonal spreading sequence with the spreading factor SF and $c_{scr}(t)$ is a common scramble sequence. $\lfloor x\rfloor$ represents the largest integer smaller than or equal to x.

B. ICI Cancellation and Despreading

ICI cancellation is performed as

$$\tilde{R}^{(i)}(k)=\hat{R}^{(i)}(k)-\tilde{M}^{(i)}(k), \quad (6)$$

where $\tilde{M}^{(i)}(k)$ is the replica of the residual ICI. $\tilde{M}^{(i)}(k)$ is given by [13]

$$\tilde{M}^{(i)}(k)=\begin{cases}0 & \text{for } i=0\\ \left\{\hat{H}^{(i)}(k)-A^{(i)}\right\}\tilde{S}^{(i-1)}(k) & \text{for } i>0\end{cases}, \quad (7)$$

where $\tilde{S}^{(i-1)}(k)$ is the kth frequency component of the replica of $s(t)$, which is generated by feeding back the (i–1)th MAP decoding result. $A^{(i)}$ is given by

$$A^{(i)}=\frac{1}{N_c}\sum_{k=0}^{N_c-1}\hat{H}^{(i)}(k). \quad (8)$$

N_c-point IFFT is applied to transform the frequency-domain signal $\{\tilde{R}^{(i)}(k); k=0\sim N_c-1\}$ into the time-domain chip block $\{\tilde{r}^{(i)}(t); t=0\sim N_c-1\}$ as

$$\tilde{r}^{(i)}(t)=\frac{1}{N_c}\sum_{k=0}^{N_c-1}\tilde{R}^{(i)}(k)\exp\left(j2\pi t\frac{k}{N_c}\right). \quad (9)$$

Despreading is carried out on $\tilde{r}^{(i)}(t)$ as

$$\hat{d}_u^{(i)}(m)=\frac{1}{SF}\sum_{t=mSF}^{(m+1)SF-1}\tilde{r}^{(i)}(t)c_u^*(t \bmod SF)c_{scr}^*(t). \quad (10)$$

C. MAP Decoding

U parallel sequences { $\hat{d}_u^{(i)}(m)$; m=0~N_c/SF–1}, u=0~U–1, are transformed into a single sequence $\left\{\hat{d}^{(i)}(n); n=0\sim K-1\right\}$ with $K=UN_c/SF$ by parallel-to-serial (P/S) conversion. Then, the log likelihood ratios (LLRs) $\Lambda_n(x)$, n=0~K–1, x=0~($\log_2 M$)– 1 (M is the modulation level), is computed as [14]

$$\Lambda_n(x)\approx\frac{\left|\hat{d}^{(i)}(n)-A^{(i)}d_{b_{n,x}=0}^{\min}\right|^2}{2\hat{\sigma}^2}-\frac{\left|\hat{d}^{(i)}(n)-A^{(i)}d_{b_{n,x}=1}^{\min}\right|^2}{2\hat{\sigma}^2}, \quad (11)$$

where $b_{n,x}$ represents the xth bit in the nth symbol and $d_{b_{n,x}=0}^{\min}$ (or $d_{b_{n,x}=1}^{\min}$) is the most probable symbol that gives the minimum Euclidean distance from $\hat{d}^{(i)}(n)$ among all the candidate symbols with $b_{n,x}=0$ (or 1) and $2\hat{\sigma}^2$ is the variance of the noise plus residual ICI.

MAP decoder is illustrated in Fig. 2. In this paper, Log-MAP algorithm is used [15]. After S/P conversion, $\mathbf{\Lambda}^{(i)}=\{\Lambda_n(x); n=0\sim K-1, x=0\sim \log_2 M-1\}$ is decomposed into three LLR sequences, $\mathbf{\Lambda}_s^{(i)}$, $\mathbf{\Lambda}_{p1}^{(i)}$ and $\mathbf{\Lambda}_{p2}^{(i)}$, associated with the information bit, the 1st parity bit and the 2nd parity bit, respectively. In the first MAP decoder, *a posteriori* LLR sequence $\boldsymbol{\lambda}^{(i)}=\{\lambda_x^{(i)}(n); n=0\sim K-1, x=0\sim \log_2 M-1\}$ is computed using $\mathbf{\Lambda}_s^{(i)}$, $\mathbf{\Lambda}_{p1}^{(i)}$ and *a priori* LLR sequence $\tilde{\boldsymbol{\lambda}}_{s2}^{(i-1)}$ ($\tilde{\boldsymbol{\lambda}}_{s2}^{(i-1)}$ is obtained from the 2nd MAP decoder in the (i–1)th iteration) as

$$\lambda_x^{(i)}(n) = \ln \frac{p(b_{n,x}=1 \mid \mathbf{\Lambda}_s^{(i)}, \mathbf{\Lambda}_{p1}^{(i)})}{p(b_{n,x}=0 \mid \mathbf{\Lambda}_s^{(i)}, \mathbf{\Lambda}_{p1}^{(i)})} \quad ,(12)$$

where $p(b_{n,x}=1\,(\text{or } 0) \mid \mathbf{\Lambda}_s^{(i)}, \mathbf{\Lambda}_{p1}^{(i)})$ is the *a posteriori* probability of $b_{n,x}=1$ (or 0) for the given $\mathbf{\Lambda}_s^{(i)}$ and $\mathbf{\Lambda}_{p1}^{(i)}$.

The *a posteriori* LLR sequence $\boldsymbol{\lambda}^{(i)}$ for the information bit sequence is denoted by $\boldsymbol{\lambda}_{s1}^{(i)}$ and that for the parity bit sequence is denoted by $\boldsymbol{\lambda}_{p1}^{(i)}$. After $\tilde{\boldsymbol{\lambda}}_{s2}^{(i-1)}$ and $\mathbf{\Lambda}_s^{(i)}$ are subtracted from $\boldsymbol{\lambda}_{s1}^{(i)}$, interleaving is applied to generate the *a prior* LLR $\tilde{\boldsymbol{\lambda}}_{s1}^{(i)}$. In the 2nd MAP decoder, using $\mathbf{\Lambda}_s^{(i)}$, $\mathbf{\Lambda}_{p2}^{(i)}$ and $\tilde{\boldsymbol{\lambda}}_{s1}^{(i)}$, the *a posteriori* LLR sequences, $\boldsymbol{\lambda}_{s2}^{(i)}$ and $\boldsymbol{\lambda}_{p2}^{(i)}$, associated with the information bit sequence and the 2nd parity bit sequence are computed. In the turbo equalization, the resulting LLR sequences, $\boldsymbol{\lambda}_{s2}^{(i)}$, $\boldsymbol{\lambda}_{p1}^{(i)}$ and $\boldsymbol{\lambda}_{p2}^{(i)}$, are P/S converted and channel de-interleaved to transform into a single *a prior* LLR sequence $\hat{\boldsymbol{\lambda}}^{(i)} = \{\hat{\lambda}_x^{(i)}(n); n=0\sim K-1, x=0\sim \log_2 M-1\}$ for MMSE weight updating and ICI cancellation for the next iteration (the (i+1)th iteration). $\hat{\lambda}_x^{(i)}(n)$ is defined as [15]

$$\hat{\lambda}_x^{(i)}(n) = \ln\left(\frac{p^{(i)}(b_{n,x}=1)}{p^{(i)}(b_{n,x}=0)}\right) \quad ,(13)$$

where $p^{(i)}(b_{n,x}=1\,(\text{or } 0))$ is the *a posteriori* probability of $b_{n,x}=1$ (or 0).

After a series of MMSE-FDE, ICI cancellation, and MAP decoding has been repeated a sufficient number of times, the received data sequence is recovered using $\boldsymbol{\lambda}_{s2}^{(i)}$. If any error is detected, the (q+1)th retransmission is requested.

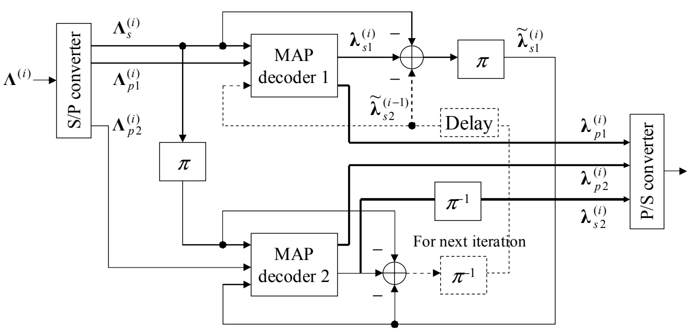

Figure 2. MAP decoder.

III. ICI Replica Generation and MMSE Weight Computation

ICI replica generation for the ith iteration and the MMSE weight computation taking into account the residual ICI are presented.

A. ICI Replica Generation

The decision variable $\tilde{d}^{(i-1)}(n)$, n=0~$K-1$, can be obtained using [11]

$$\tilde{d}^{(i-1)}(n) = \sum_{d\in D} d \prod_{b_{n,x}\in d} p^{(i-1)}(b_{n,x}) \quad ,(14)$$

where d represents the candidate symbol having $b_{n,x}=0$ or $b_{n,x}=1$ in the symbol set D and $p^{(i-1)}(b_{n,x}=0)$ and $p^{(i-1)}(b_{n,x}=1)$ are given, from Eq. (13), by

$$p^{(i-1)}(b_{n,x}) = \begin{cases} -\frac{1}{2}\tanh\left(\frac{\hat{\lambda}_x^{(i-1)}(n)}{2}\right)+\frac{1}{2} & \text{for } b_{n,x}=0 \\ \frac{1}{2}\tanh\left(\frac{\hat{\lambda}_x^{(i-1)}(n)}{2}\right)+\frac{1}{2} & \text{for } b_{n,x}=1 \end{cases} \quad (15)$$

since $p^{(i-1)}(b_{n,x}=1)+p^{(i-1)}(b_{n,x}=0)=1$.

$\tilde{d}^{(i-1)}(n)$ in Eq. (14) is the expectation of the transmitted symbol and is used as the soft symbol replica as in [11]. For QPSK data modulation and 16QAM, $\tilde{d}^{(i-1)}(n)$ is

$$\tilde{d}^{(i-1)}(n) = \begin{cases} \frac{1}{\sqrt{2}}\tanh\left(\frac{\hat{\lambda}_0^{(i-1)}(n)}{2}\right) + j\frac{1}{\sqrt{2}}\tanh\left(\frac{\hat{\lambda}_1^{(i-1)}(n)}{2}\right) \\ \qquad \text{for QPSK} \\ \frac{1}{\sqrt{10}}\tanh\left(\frac{\hat{\lambda}_0^{(i-1)}(n)}{2}\right)\left\{2+\tanh\left(\frac{\hat{\lambda}_1^{(i-1)}(n)}{2}\right)\right\} \\ \quad + j\frac{1}{\sqrt{10}}\tanh\left(\frac{\hat{\lambda}_2^{(i-1)}(n)}{2}\right)\left\{2+\tanh\left(\frac{\hat{\lambda}_3^{(i-1)}(n)}{2}\right)\right\} \\ \qquad \text{for 16QAM} \end{cases} \quad .(16)$$

After transforming { $\tilde{d}^{(i-1)}(n)$; n=0~K–1} into U parallel sequences { $\tilde{d}_u^{(i-1)}(m)$; m=0~N_c/SF}, u=0~U–1, the replica $\{\tilde{s}^{(i-1)}(t); t=0\sim N_c-1\}$ for the transmitted chip sequence $s(t)$ is generated as

$$\tilde{s}^{(i-1)}(t) = \left[\sum_{u=0}^{U-1} \tilde{d}_u^{(i-1)}(\lfloor t/SF \rfloor) c_u(t \bmod SF)\right] c_{scr}(t) \quad .(17)$$

After block chip-interleaver is applied to $\tilde{s}^{(i-1)}(t)$ to randomize burst errors (SF consecutive errors) which appear in $\tilde{s}^{(i-1)}(t)$, { $\tilde{s}^{(i-1)}(t)$;t=0~N_c–1} is transformed by N_c-point

FFT into the frequency-domain signal $\{\widetilde{S}^{(i-1)}(k)$;k=0~(N_c–1)} as

$$\widetilde{S}^{(i-1)}(k)=\sum_{t=0}^{N_c-1}\widetilde{s}^{(i-1)}(t)\exp\left(-j2\pi k\frac{t}{N_c}\right) .(18)$$

Substituting Eq. (18) into Eq. (7), the frequency-domain ICI replica $\widetilde{M}^{(i)}(k)$ is obtained.

B. MMSE Weight

At the first iteration (i=0), MMSE-FDE is performed before ICI cancellation. Since the residual ICI is suppressed by ICI cancellation, the MMSE weight needs to be updated in each iteration (i>0). In this paper, the MMSE weight, taking into account the residual ICI, is derived for each iteration. To derive the MMSE weight, we define the equalization error $e(k)$ between $\widetilde{R}^{(i)}(k)$ after ICI cancellation and $S(k)$ as

$$e(k)=\widetilde{R}^{(i)}(k)-A^{(i)}S(k) \text{ , (19)}$$

where $A^{(i)}S(k)$ is used as the reference since $E[\widetilde{R}^{(i)}(k)]=A^{(i)}S(k)$ (the residual ICI is assumed to be zero-mean). $w_{q'}^{(i)}(k)$, $q'=1,2,...,q$, is the weight that minimizes the mean square error (MSE) $E[|e(k)|^2]$ for the given $H(k)$, i.e., $\partial E[|e(k)|^2]/\partial w_{q'}^{(i)}(k)=0$. The following MMSE weight is obtained:

$$w_{q'}^{(i)}(k)=\frac{H^{(q')}(k)}{\rho^{(i-1)}\sum_{q'=1}^{q}\left|H^{(q')}(k)\right|^2+2\sigma^2} \text{ , (20)}$$

where $2\sigma^2=2N_cN_0/T_c$ is the noise variance with N_0 being the single-sided power spectrum density of the additive white Gaussian noise (AWGN). $\rho^{(i-1)}$ is given by

$$\rho^{(i-1)}=SF\sum_{m=0}^{N_c/SF-1}\sum_{u=0}^{U-1}\left\{E\left[|d_u(m)|^2\right]-\left|\widetilde{d}_u^{(i-1)}(m)\right|^2\right\}. \text{ (21)}$$

$E[|d_u(m)|^2]$ is obtained as follows. First, $E[|d(n)|^2]$ is computed, using Eq. (15) as

$$E[|d(n)|^2]=\sum_{d\in D}|d|^2\prod_{b_{n,x}\in d}p^{(i-1)}(b_{n,x})$$
$$=\begin{cases}1 & \text{for QPSK}\\ \frac{4}{10}\tanh\left(\frac{\hat{\lambda}_1^{(i-1)}(n)}{2}\right)+\frac{4}{10}\tanh\left(\frac{\hat{\lambda}_3^{(i-1)}(n)}{2}\right)+1 & \text{for 16QAM}\end{cases} \text{ . (22)}$$

Then, $\{E[|d(n)|^2]$; n=0~K–1} is transformed into U parallel sequences to get $\{E[|d_u(m)|^2]$; m=0~N_c/SF}, u=0~U–1.

IV. COMPUTER SIMULATION RESULT

We consider HARQ Type I [1]. A turbo encoder with (13,15) RSC encoders and a decoder with Log MAP algorithm are used. Turbo code with a constraint length of 4 is assumed. The length of the coded bit sequence is 2048 bits. The code rate is assumed to be R=1/2 and 3/4. We assume QPSK 16QAM data modulation, N_c=256 chips and N_g=32-chip GI. The channel is assumed to be a frequency-selective block Rayleigh fading channel having a chip-spaced L=16-path uniform power delay profile [8]. The lth path time delay (l=0~L–1) is assumed to be l chips. Perfect chip timing and ideal channel estimation are assumed. The number of iterations in the turbo equalization is set to 6. The maximum number of packet retransmissions is set to 100.

The simulated HARQ throughput performance of DS-CDMA with MMSE turbo equalization is plotted in Fig. 3 as a function of the average received symbol energy-to-AWGN noise power spectrum density ratio E_s/N_0 for SF=U=16. For comparison, the HARQ throughput performances of DS-CDMA without turbo equalization and rake combining and that of OFDM are also plotted (OFDM with N_c=256 subcarriers and N_g=32-sample GI is assumed). MMSE turbo equalization improves the throughput performance since it can suppress the residual ICI while achieving a higher coding gain. For 16QAM, the Euclidean distance between different symbols is shorter and hence, decision error due to the residual ICI is more likely than for QPSK. Therefore, the use of MMSE turbo equalization is more effective to improve the throughput for 16QAM than for QPSK. An E_s/N_0 reduction of about 2.5~3 dB can be achieved for a throughput range of 2~2.5 bit/s/Hz. Rake combining exhibits very poor throughput performance due to the large IPI.

It can be seen from Fig. 3 that HARQ throughput of DS-CDMA with MMSE turbo equalization is higher than that of OFDM for E_s/N_0>13dB and E_s/N_0<9 dB. In an E_s/N_0 region of 9~13 dB, the throughput of DS-CDMA is slightly worse than OFDM.

V. CONCLUSION

In this paper, MMSE turbo equalization was introduced into type I HARQ using multicode DS-CDMA and the throughput performance was evaluated by computer simulation. The MMSE turbo equalization improves the HARQ throughput since it can successfully suppress the residual ICI while achieving higher coding gain. It was shown that DS-CDMA with MMSE turbo equalization gives higher throughput or almost the same throughput as OFDM.

REFERENCES

[1] D. Garg and F. Adachi, "Comparison of Rcpt HARQ Throughpyt Using OFDM, MC-CDMA and DS-CDMA with Frequency-domain Equalization," Proc. 9th IEEE ICCS 2004, Singapore, 6-8 Sep, 2004.

[2] *Physical layer aspects of UTRA High Speed Downlink Packet Access* (Release 4), Mar. 2001. 3GPP, 3G TR25.848 V4.0.0.

[3] W. C., Jakes Jr., Ed., *Microwave mobile communications*, Wiley, New York, 1974.

[4] J. G. Proakis, *Digital communications*, 3rd ed., McGraw-Hill, 1995.

[5] F. Adachi, M. Sawahashi, and H. Suda, "Wideband DS-CDMA for next generation mobile communications systems," IEEE Commun. Mag., vol. 36, pp.56-69, Sept. 1998.
[6] F. W. Vook, T. A. Thomas, and K. L. Baum, "Cyclic-prefix CDMA with antenna diversity," Proc. IEEE VTC02-Spring, pp. 1002-1006, May 2002.
[7] F. Adachi, T. Sao, and T. Itagaki, "Performance of multicode DS-CDMA using frequency domain equalization in a frequency selective fading channel," Electronics Letters, Vol. 39, pp.239-241, Jan. 2003.
[8] F. Adachi, D. Garg, S. Takaoka, and K. Takeda, "Broadband CDMA techniques," IEEE Wireless Commun. Mag., Vol. 12, No. 2, pp. 8-18, April. 2005.
[9] I. Martoyo, G. M.A. Sessler, J. Luber and F. K. Jondral, "Comparing equalizers and multiuser detections for DS-CDMA downlink systems," Proc. IEEE VTC 2004-Spring, 17-19 May 2004.
[10] D. Raphaeli and Y. Zarai, "Combined turbo equalization and turbo decoding," IEEE Commun. Letters, Vol. 2, No. 2, pp. 107-109, April 1998.
[11] X. Wang and H. V. Poor, "Iterative (turbo) soft interference cancellation and decoding for coded CDMA," IEEE Commun. Mag., Vol. 47, No.7, pp.1046-1060, July 1999.
[12] C. Laot, R. L. Bidan, and D. Leroux, "Low-complexity MMSE Turbo Equalization: a possible solution for EDGE," IEEE. Trans. Wire. Commun., Vol. 4, No. 3, pp.965-974, May 2005.
[13] K. Takeda and F. Adachi, "MMSE turbo equalization for multicode DS-CDMA," Proc. 10th IEEE International Conference on Communications Systems (ICCS 2006), Singapore, 30 Oct.-1 Nov. 2006.
[14] A. Stefanov and T. Duman, "Turbo coded modulation for wireless communications with antenna diversity," Proc. IEEE VTC99-Fall, pp.1565-1569, Netherlands, Sept. 1999.
[15] J. P.Woodard and L. Hanzo, "Comparative study of turbo decoding techniques: An overview", IEEE Trans. Veh. Technol., Vol.49, pp.2208-2233, Nov. 2000.

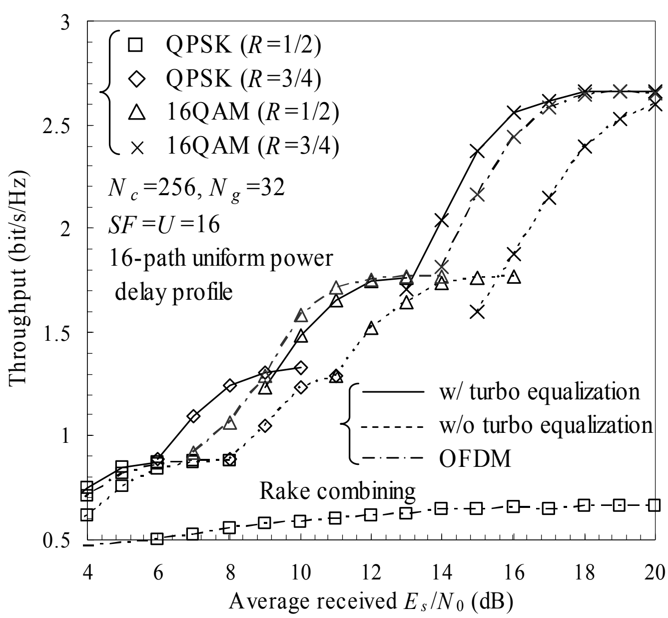

Figure 3. HARQ throughput performance.